

# Highly Sensitive Detection of Trace Gases Using The Time Resolved Frequency Down-chirp From Pulsed Quantum-Cascade Lasers

Michael T. McCulloch, Erwan L. Normand,

Nigel Langford and Geoffrey Duxbury<sup>a</sup>

Department of Physics and Applied Physics, University of Strathclyde, John Anderson Building, 107 Rottenrow, Glasgow, G4 0NG, UK.

D. A. Newnham

Space Science Department, Rutherford Appleton Laboratory, Chilton, Didcot, Oxfordshire, OX11 0QX, UK.

## 1. ABSTRACT

A spectrometer using a pulsed, 10.25 microns wavelength, thermoelectrically cooled quantum-cascade distributed-feedback laser has been developed for sensitive high-resolution infrared absorption spectroscopy. This spectrometer is based upon the use of the almost linear frequency down- chirp of up to 75 GHz produced by a square current drive pulse. The behaviour of this down-chirp has been investigated in detail using high resolution Fourier transform spectrometers. The down-chirp spectrometer provides a real-time display of the spectral fingerprint of molecular gases over a wavenumber range of up to  $2.5 \text{ cm}^{-1}$ . Using an astigmatic Herriott cell with a maximum path length of 101 m,

and a 5 kHz pulse repetition rate with 12 second averaging, absorption lines having an absorbance of less than 0.01, (an absorption of less than 1%) may be measured.

Keywords: Laser Physics; Laser sources; Atomic and molecular spectroscopy; Gas sensing

<sup>a</sup> corresponding author, E-mail [G.Duxbury@strath.ac.uk](mailto:G.Duxbury@strath.ac.uk), Telephone 0044-141-548-3271

## 2. INTRODUCTION

Recent advances in the fabrication of pulsed quantum-cascade (QC) lasers have allowed the development of lasers that work at or close to room temperature whilst producing pulses with peak powers that are in excess of 1 Watt with duty cycles approaching 100%.<sup>1,2</sup> The operating wavelength associated with QC lasers falls typically in the 3 – 15  $\mu\text{m}$  window and so makes the QC laser an ideal light source for probing the spectral features associated with the fundamental vibration-rotation absorption bands of gaseous molecules, as was discussed recently by Kosterev and Tittel<sup>3</sup>. They have reviewed many of the ways in which QC based spectrometers are, or may be developed, for highly sensitive trace gas sensing in our atmosphere. Spectrometers for the detection of atmospheric trace gases must fulfil two main requirements: to be able to record an identifiable molecular fingerprint; to be able to detect very small atmospheric concentrations. Both of these requirements are fulfilled by the spectrometer described in this paper.

In atmospheric spectroscopy trace molecules may be detected using both Fourier transform and by laser based spectrometers<sup>4</sup>. Fourier transform instruments have been widely used for ground, airborne and space-borne measurements<sup>4</sup>. They have very wide wavelength coverage and may have very high spectral resolution. These instruments may be used in solar occultation mode, with starlight, or to analyse directly emission from molecules in the atmosphere. Normally interferometric spectrometers do not offer the fast time resolution of laser based spectrometers.

Diode laser absorption spectrometers have been developed for two main regions, the near-infrared region from about 1 to 2.2  $\mu\text{m}$ , and the mid-infrared region from 3 to 15  $\mu\text{m}$ . The near infrared systems make use of diode lasers developed as part of the spinout from telecommunications laser development, and are excellent for detecting the vibrational overtone bands of small molecules containing CH or OH bonds such as methane or water. Since the lasers and detectors may be cooled thermoelectrically, very lightweight spectrometer designs are possible<sup>4</sup>. For most molecules the mid-infrared region is more desirable owing to the greater transition moments. Several sensitive spectrometers based upon narrow linewidth semiconductor lead salt lasers and long path length absorption

cells, such as the ALIAS family,<sup>5,6</sup> developed by Webster's group, have been successfully deployed on aircraft and on balloons for atmospheric sensing.

One way in which continuously operating quantum-cascade lasers, operating at cryogenic temperatures, may be used is as a "drop in" replacement for a lead salt laser in such a system. The recent work of Webster and his colleagues exemplifies the success of this approach<sup>3</sup>. Since the quantum-cascade lasers appear to possess better temperature cycling behaviour, and their centre frequencies are little affected by small temperature variations of the substrate, for some types of system the use of cryogenically cooled devices is an attractive option.

However, for convenience, and to reduce the overall weight of the system, it is often better to operate a spectrometer source at temperatures close to room temperature. At present in order to operate a QCL without cryogenic cooling it is necessary to operate in current-pulsed mode. Most of the present generation of QC laser based spectrometers<sup>2,7,8</sup> operate in a manner similar to that initiated by Namjou et al.<sup>7</sup> In these systems a short duration current pulse ( $\sim 3$  to  $10$  ns) is applied to the QC laser and this results in the generation of a pulse in the spectral domain, which covers a given wavenumber/cm<sup>-1</sup> range, so that a single spectral element is recorded in each pulse. This spectral element is then tuned through the absorption feature of interest by applying a slowly varying sub-

threshold current ramp to the pulse train. As a result the observed frequency tuning is a quadratic function of the applied current ramp. Using this technique spectral scans over the range of  $0.22 \text{ cm}^{-1}$  to  $0.74 \text{ cm}^{-1}$ <sup>2,5</sup> have been achieved. To cover a larger frequency range slow temperature scanning is used. In a recent instrument described by Kosterev et al.<sup>8</sup>, a fast scan of  $0.22 \text{ cm}^{-1}$  is combined with the option of slow  $2.5 \text{ cm}^{-1}$  scans. They have also described the calibration of the fast scan to take into account the effects of the quadratic frequency chirp. In both fast and slow scan modes sophisticated computer controlled pulse sequences were employed. In this type of spectrometer the resolution limit is set by the effective linewidth of the current pulse emitted by the laser.

Our approach to measuring the spectral fingerprint of a given molecular gas differs significantly to the approach outlined above and is characterised by the simplicity of the method. The design of our spectrometer has its origin in the results of our characterisation of the spectral behaviour of pulsed quantum-cascade lasers using high resolution continuously scanning Fourier transform spectrometers.<sup>9</sup> By analysing the wavenumber profile of the output pulse, and by varying the duration of the current pulse, we have shown that, when a top-hat current pulse is applied to a QC laser, the laser frequency tunes almost linearly to lower wavenumber (lower frequency) as a function of time. This is referred to a wavenumber (or frequency) down-chirp. This down-chirp may cover a wavenumber region of up to  $2.5 \text{ cm}^{-1}$ , and hence may be used to scan the

oscillating frequency through the molecular transitions of interest<sup>10</sup>. The principal advantages of the wavenumber down-chirp method in comparison with the short pulse approach are the following:

All spectral elements are recorded during a single laser pulse;

A much wider fast tuning range is accessible;

The wavenumber tuning is a much more linear function of the scan time.

The resolution limitations of both the short pulse and the wavenumber down-chirp methods are similar, and are set by the transform limit of the pulse<sup>8,11</sup>, or of the bandwidth- time duration product of the signal detected by the fast detection system<sup>12</sup>.

This is sometimes referred to as the “uncertainty-relation”<sup>12</sup>.

In their assessment of the resolution limitations of their short-pulse spectrometer, Kosterev and his colleagues about 75% of the laser energy lies in the transform limited part of the spectrum of the pulsed output. By analysing the line shapes of their spectra they have demonstrated that a full width at half maximum (FWHM) of  $9.5 \times 10^{-3} \text{ cm}^{-1}$  (290 MHz) may be achieved. They have also shown that care is needed to lessen the effects of energy in the tail of the laser pulse.

The resolution of our time-resolved spectrometer is not determined by the effective line width of the laser induced by the current pulse, but by the chirp rate of the laser and the temporal resolution of the detection system. In both the short pulse and in the wavenumber down-chirp spectrometers, the bandwidth-duration product of a signal cannot be less than a certain minimum value, the "uncertainty relation". This relationship is described in detail by Bracewell<sup>12</sup>, who has given the proof that the product of the equivalent duration,  $t$ , and the equivalent bandwidth,  $\nu$ , must exceed or be equal to  $C$ , a constant that is determined by the pulse shape. For a rectangular time window  $t \nu C = 0.886$ , and for a Gaussian time window  $t \nu C = 0.441$ . In the description of their short pulse spectrometer Kosterev et al.<sup>8</sup> have shown that their resolution of 290 MHz cannot be significantly improved by changing the pulse duration. If the pulse duration were to be shortened there would be a Fourier transform limitation to the resolution, whereas if it were to be lengthened the frequency chirp would be excessive. A similar analysis may be carried out for the limitations of the time resolved detection system, as outlined below.

In a time window  $\tau$  the laser frequency will chirp by the amount  $d\nu/dt \tau$ , so that if a smaller time window were to be used the Fourier-limited frequency interval  $\nu$  would increase, whereas the chirp limited frequency interval would decrease. The best aperture

time,  $\tau$ , will therefore be determined by  $C/\tau = dv/dt \tau$ . Rewriting this equation in terms of  $\nu$  gives,  $\nu = dv/dt C/\nu$ , from which  $\nu = \sqrt{Cdv/dt}$ . In the limiting case of  $C=1$ , and a chirp rate of 200 MHz/ns, the limit of resolution would be 447 MHz, (or  $0.015 \text{ cm}^{-1}$ ). This would fall to 421 MHz ( $0.014 \text{ cm}^{-1}$ ) if the rectangular window function is used, and to 297 MHz ( $0.01 \text{ cm}^{-1}$ ) if a Gaussian time window is appropriate. As Kosterev and his colleagues have noted<sup>8</sup> a significant improvement of the resolution would require the design and fabrication of lasers with decreased thermal dissipation within their structure, in order to reduce the wavenumber down-chirp rate. In this paper we will show evidence for the improvement of resolution of the down-chirp spectrometer when the chirp rate is slowed.

### **3. CHARACTERISATION OF PULSED QUANTUM-CASCADE LASERS**

#### **3.1 EXPERIMENTAL**

The experimental configuration for laser characterization is shown in a previous paper<sup>10</sup>. For the results described here, the QC laser, fabricated by Alpes Lasers, had a distributed feedback (DFB) structure, and was designed to oscillate at a wavelength of  $10.2 \mu\text{m}$ . The laser was housed in airtight chamber, and the light was coupled from the chamber through an anti-reflection coated ZnSe window. The QC laser substrate was mounted on a Peltier cooler, which allowed the substrate temperature to be varied

between  $-40^{\circ}\text{C}$  and  $+40^{\circ}\text{C}$ . The temperature of the substrate was stabilised to a level of  $\pm 0.01^{\circ}\text{C}$ .

The laser was excited using pulsed current source designed within our group. This generated top-hat shaped current pulses with durations ranging from 40 ns to 300 ns, at repetition rates of up to 100 kHz and with peak currents of up to 6 A. The amplitude and shape of the current pulse applied to the QC laser were monitored using a Rogowski coil<sup>9</sup> placed between the current source and the QC laser. The threshold current of the QC laser was 3.2 A at a substrate temperature of  $0^{\circ}\text{C}$ .

The spectral profile of radiation produced by the QC laser was studied by use of two Fourier transform spectrometers, a Bomem DA-3 FTS which had a maximum effective resolution of  $0.005\text{ cm}^{-1}$ , (150 MHz), and a Bruker IFS 120HR with a maximum resolution of  $0.0015\text{ cm}^{-1}$ , (45 MHz). Once a numerical filter is applied to the interferogram, the maximum sampling frequency of these spectrometers is very much less than the repetition frequency of the current pulses applied to the QC laser (20 – 100 kHz), hence the QC laser appears as a quasi-continuous-wave light source when viewed by the FT spectrometers.

Previous measurements that we have made using this laser<sup>9</sup> indicate that, when the drive pulse amplitude is 5 A, by varying the temperature of the QC laser substrate, the oscillating wave number can be tuned at a rate of  $-7.6 \times 10^{-2} \text{ cm}^{-1}/\text{K}$ , which corresponds to a frequency down-chirp of 2.3 GHz/K.

In a previous paper <sup>9</sup>, for which Bomem DA-3 FT spectrometer (FTS) was used, we showed that when a current pulse of 100 ns duration was applied to the laser the wavenumber/ $\text{cm}^{-1}$  down-chirp was almost linear. By using the higher resolution Bruker spectrometer in the NERC Molecular Spectroscopy Facility (MSF) at Rutherford Appleton Laboratory (RAL) we have been able to further characterize the pulse structure, and to examine the pattern of molecular fingerprint absorption lines which lie within the tuning range of the present laser. In Figures 1(a) an example is shown of the high resolution absorption spectrum of 1,1 difluoroethylene,  $\text{CF}_2\text{CH}_2$  recorded using the Bruker FTS with the QCL as the source. As we have described in detail recently<sup>10</sup>, since the linewidth of this spectrum determined by the instrument function of the FTS, it can be seen that the effective linewidth of the wavenumber swept QCL, when recorded using a slow detection system which acts as a time integrator, must be less than 45 MHz.

From Fig1(a) it may also be seen that the effects of the switch on of the current pulse are to produce a very fast transient oscillation of the output power which damps rapidly, so

that over most of the current pulse the envelope of the laser output has an approximately trapezoidal shape. It is this part of the output pulse that we use to provide the basis of our QCL spectrometer<sup>9</sup>.

#### **4. IMPLEMENTATION OF A FAST REAL-TIME SPECTROMETER**

##### **4.1 EXPERIMENTAL DESIGN**

The experimental arrangement of our spectrometer is shown in Figure 2. The output from a distributed feedback QC laser, described in section 1.1, was collected and collimated by an off-axis parabolic mirror-germanium telescope arrangement to produce a beam of diameter 3 mm which was subsequently passed, via a set of steering mirrors, into a multiple pass cell. In our original system the cell used was a White cell<sup>10</sup>, but for the experiments described in the present paper an astigmatic Herriott Cell<sup>13</sup> has been used. After traversing this cell the light is then focussed onto a high-speed photovoltaic mercury-cadmium-telluride (MCT) detector<sup>15</sup>. The output from this detector is then amplified and coupled to a digital oscilloscope. The spectra recorded via this oscilloscope may be used, in conjunction with a stored background trace, to provide real time transmission spectra. Currently the original and the processed spectra are stored for further off-line processing. However, in the next generation spectrometer the signal acquisition system will be integrated with the control computer.

To avoid signal distortion, the detector amplifier used has a bandwidth of 1.1 GHz<sup>16</sup>. The effective bandwidth of the detection system comprising the detector amplifier and digitiser was determined to be greater than 400 MHz. The resultant temporal resolution of this system is about 1.35 ns. This temporal resolution is essential for the operation of our spectrometer. We have also developed efficient electrical screening of the detector amplifier system, leading to the removal most of the effects of electrical pickup associated with the proximity of the pulse generation system to the detection system.

In the series of experiments described in the present paper, we have used an astigmatic Herriott cell whose mirrors were originally designed by Howieson<sup>11</sup>. The Herriott cell mirrors were separated by approximately 0.5 m, and were initially used with 36 passes, leading to an effective path length of approximately 18 m, and finally with 202 passes, an effective path length of approximately 101 metres. The ray tracing software used to model the behaviour of this cell has been developed within our group by McCulloch and Walker, and is based on the method of McManus et al.<sup>13</sup>.

The success of the spectrometer relies upon the fast response time of the detector amplifier combination, and upon rapid digitisation of the signal from the amplifier. Examples of typical detector signals of background laser pulses are shown in Figure 3. In 3(a) where an optical path length of 18 m was used some interference between the pulse generator and the signal pulse may be seen, whereas in 3(b) where the signal pulse is

delayed owing to 101 m path length used, the effects of electrical pickup are absent from the signal region of the output of the detector.

We have already seen in the spectra recorded via the Fourier transform spectrometers, Figure 1(a), and measured directly, Figure 1(b), that once the initial part of the emitted pulse containing ringing associated with the switching transient is passed, the remainder of the output pulse of the QC laser has an approximately trapezoidal shape. In our first series of measurements, we determined the rate of wavenumber chirp by comparing the time dependence of the measured fringe spacings of the two germanium etalons, one nominally  $0.02 \text{ cm}^{-1}$  and the other nominally  $0.05 \text{ cm}^{-1}$ . Assuming a linear dependence of chirp with time, the rate of change of wavenumber as a function of pulse duration, using a pulse repetition frequency of 500 Hz, and a drive current of 5 A, was determined to be 260 MHz/ns ( $8.7 \times 10^{-3} \text{ cm}^{-1}/\text{ns}$ ).

However, when the temporal separation of the etalon fringes was analysed, it was found that for pulses of length up to 200ns a small quadratic correction is required, and for longer pulses of up to 300 ns a very small cubic correction is also necessary. Absolute wavenumber calibration has been achieved using the  $\text{CF}_2\text{CH}_2$  absorption lines in groups (i) (ii) and (iii), shown in Fig. 1, which have been calibrated making use of the high resolution Fourier transform absorption spectrum shown in Figure 1(a). The quality of the

temporal resolution of the detection system may be inferred from the resolution of the closely spaced absorption lines of  $\text{CF}_2\text{CH}_2$  displayed in Figure 1(b).

## 4.2 RESULTS

In the design of instrumentation for the detection of atmospheric trace gases there are two main requirements, the ability to recognise an identifiable molecular fingerprint and the need to detect very small atmospheric concentrations. In this section we will first of all consider the ability of the spectrometer to deliver spectra in which the unique signatures of individual molecules are readily identified, and secondly the high sensitivity of this type of spectrometer for detecting trace concentrations of atmospheric gases.

## 4.3 MOLECULAR SPECTRA FINGERPRINT RECOGNITION

Most spectrometers used for detecting atmospheric trace gases rely on exploiting the micro-windows within which there are few interfering absorption lines of water and carbon dioxide<sup>4</sup>. These micro windows may be quite wide, up to  $50\text{ cm}^{-1}$  but are frequently quite narrow,  $1\text{ to }3\text{ cm}^{-1}$ . As we have shown above, provided the pulse current amplitude is fixed, for a given sub-microsecond pulse duration and drive current, the usable width of the wavenumber down-chirp is almost linear across this window and may be up to  $2.5\text{ cm}^{-1}$ , comparable to that used in other remote sensing systems.<sup>2,4,8</sup> We will

also demonstrate that the achievable spectral resolution,  $\nu$ , approaches that set by the "uncertainty relation" discussed in the introduction,  $\nu = C/\tau = \sqrt{Cdv/dt}$ . These two features mean that we should be able to make a direct measurement of the absorption bands of any molecular gas that absorbs within the wave number region covered by a given QC laser without having to step tune the laser through the absorption band.

The gases which we have chosen to use to illustrate effectiveness of the micro-window approach using our spectrometer are carbonyl fluoride,  $\text{COF}_2$  and 1,1 difluoroethylene,  $\text{CF}_2\text{CH}_2$ . These are both near-oblate asymmetric rotor molecules with very similar moments of inertia and hence very similar rotation constants. Both of the bands, which have absorption lines lying within the present tuning range of our spectrometer, are perpendicular bands of a near-oblate top<sup>4</sup>. The  $\nu_9$  band of  $\text{CF}_2\text{CH}_2$  is a *B*-type band<sup>17</sup> with selection rules  $K_a = \pm 1$ ,  $K_c = \pm 1$ , and  $J = 0, \pm 1$ , whereas the  $\nu_2$  band of  $\text{COF}_2$  is an *A*-type band<sup>18,19</sup>, with selection rules  $K_a = 0$ ,  $K_c = \pm 1$  and  $J = 0, \pm 1$ . Since the rotation constants of these two molecules are very similar, at medium resolution the spectra appear to consist of broad almost equally spaced features, with similar separations of the groups of closely spaced absorption lines in both molecules<sup>4</sup>. However at higher resolution these features are resolved to reveal a distinctive fingerprint patterns of planar, near-oblate tops within our wavenumber  $/\text{cm}^{-1}$  chirp range. It can be seen that the

structure of these features is much more irregular in the part of the  $\text{CF}_2\text{CH}_2$  absorption spectrum which lies within our micro window in comparison with the more regular patterns seen in that of  $\text{COF}_2$ .

These molecules are both examples of heavy molecules of the type found in the atmosphere. Carbonyl fluoride has been detected in the stratosphere via its infrared spectrum, and 1,1 difluoroethylene is an example of a heavy molecule which might be considered as a prototype for hydrofluorocarbon (HFC) detection, although it itself is not one of the main HFC's being emitted into the atmosphere.

In Figure 4 the transmission spectra of  $\text{COF}_2$  and  $\text{CF}_2\text{CH}_2$  are shown within a  $1.5 \text{ cm}^{-1}$  down-chirp range. The wavenumber/ $\text{cm}^{-1}$  calibration has been achieved by using our newly measured high resolution spectrum of  $\text{CF}_2\text{CH}_2$  (see section 1.2) and the spectra of the  $\nu_2$  band of  $\text{COF}_2$  recorded by Lewis-Bevan et al.<sup>16,17</sup>, and also by using spectra recorded by our Bomem FTS. At gas pressures of about 0.05 Torr, and with a drive current of current of 4.4 amps, the effective resolution is ca  $0.017 \text{ cm}^{-1}$ . If a lower drive current of 4.1 amps is used, and the other spectrometer conditions are unchanged, the rate of the wavelength chirp is slowed yielding a narrower micro-window, but the resolution is much improved to ca  $0.015 \text{ cm}^{-1}$ . This effect is shown in Figure 5. It may be noted that

even when the wider chirp-tuning is used, the resolution of the instrument is quite sufficient to discriminate between the two species, since the very different patterns within the groups may be readily identified.

Not only may the rate of down-chirp be determined by the drive current of the laser, it may also vary significantly during a long pulse, since the rate of chirp slows across the pulse. An example of this behaviour is shown in Figure 6, where transmission spectra recorded at the beginning and the end of the pulse of laser emission are compared with the equivalent part of the high resolution Fourier transform spectrum recorded using the RAL spectrometer. The rate of chirp slows appreciably from approximately -286 MHz/ns in the early part of the pulse to -239 MHz/ns in the final part. A marked difference in the resolution may be seen between the spectra recorded in this way, since the lines spaced by about  $0.01 \text{ cm}^{-1}$  in the central group of strong lines are resolved in the slow chirp 6(b), but cannot be resolved in the faster chirp of 6(c). Note that most of the lines seen in the high resolution spectrum, 6(a) may be identified in 6(b).

#### **4.4 DETECTION OF CO<sub>2</sub> AND H<sub>2</sub>O IN THE LABORATORY ATMOSPHERE.**

In order to test the sensitivity of our spectrometer we recorded a number of spectra in which the cell was filled with laboratory air up to a total pressure of 200 Torr. In Figure

7 sections of three of these spectra are shown where weak water and carbon dioxide absorption lines may be seen. In order to make a comparison with similar measurements of nitrous oxide in laboratory air<sup>8</sup> it is necessary to note the difference in the absorption line intensities, which are given in Table 1. Although the concentrations of water and carbon dioxide are much greater than those of nitrous oxide, their line intensities are much lower<sup>20,21</sup>. In the case of the R(16) line of the 00<sup>0</sup>1-10<sup>0</sup> band of CO<sub>2</sub> the weakness is due to the small thermal population of the lower state. The transition of water is weak since it involves a change of K<sub>a</sub> of 5, making it highly forbidden.<sup>20</sup> The concentration of carbon dioxide is expected to be at least a thousand times greater than that of nitrous oxide, however its absorption line intensity is approximately two and a half thousand times weaker. The clear detection of the weak carbon dioxide line, and the manner in which the carbon dioxide signal may easily be enhanced by the input of a small sample of human breath, shows the sensitivity of the wavenumber down-chirp spectrometer.

## 5. CONCLUSION

In conclusion we have demonstrated a simple real-time mid infrared spectrometer that is capable of making sensitive measurements of the concentration of molecular vapours, as well as providing a display of the molecular fingerprint associated with a particular gas. We have described the advantages of the down-chirp spectrometer, namely the detection

of the spectrum in the entire spectroscopic micro-window at every pulse, and the increased width of the micro-window in comparison with the short pulse spectrometer. We have also demonstrated that we can achieve a resolution close to the ideal achievable spectral resolution,  $\nu$ , which is determined the "uncertainty relation" discussed in the introduction,  $\nu = \sqrt{Cdv/dt}$ . Thus the resolution of both the short pulse and the wavenumber chirp spectrometers are set by the transform limit.

## 6. ACKNOWLEDGEMENTS:

The authors would like to thank the United Kingdom Engineering and Physical Sciences Research Council for the funding of this work through the research grant GST/M69111 1999. We would also like to thank the staff at the National Environmental Research Council (NERC) molecular spectroscopy Facility at the Rutherford Appleton Laboratory for their support of the first part of this project, and to Marwa Saad Moussa Alansary for her help with the spectrometer calibration. We are also grateful to Agilent, LeCroy Ltd and Acquiris for the loan of high speed digital oscilloscopes and digitisers. Finally we would also like to acknowledge the helpful comments of one of the referees on the operation of pulsed quantum-cascade laser spectrometers.

## 7. REFERENCES

1. M. Beck, D.Hofstetter, T. Aellen, J. Faist, U. Oesterle, M. Ilagems, E. Gini and H. Melchior, *Science* **295**, 301-305 (2002)
2. A.A.Kosterev and F.K. Tittel, *IEEE J Quant. Electron.* **38**, 582-591 (2002)
3. C. R. Webster, G. J. Flesch, D. C. Scott, J. E. Swanson, R. D. May, W. S. Woodward, C. Gmachl, F. Capasso, D. L. Sivco, J. N. Baillargeon, A. L. Hutchinson and A. Y. Cho, *Applied Optics* **40**, 321-326 (2001).
4. Geoffrey Duxbury, "Infrared Vibration-Rotation Spectroscopy From Free Radicals to the Infrared Sky", Wiley (2000).
5. C.R. Webster, R.D. May, C.A. Trimble, R.G. Chave and J. Kendall, *Appl. Opt.* **33**, 454-472 (1994)
6. D.C. Scott, R.L. Herman, C.R. Webster, R.D. May, G.J. Flesch and E.J. Moyer, *Appl. Opt.* **38**, 4609-4622 (1999)
7. K. Namjou, S. Cai, E. A. Whittaker, J. Faist, C. Gmachl, F. Capasso, D. L. Sivco and A. Y. Cho, *Optics Letters* **23**, 219-221 (1998).
8. A. A. Kosterev, R. F. Curl, F. K. Tittel, C. Gmachl, F. Capasso, D. L. Sivco, J. N. Baillargeon, A. L. Hutchinson and A. Y Cho, *Applied Optics* **39**, 6866-6872 (2000).
9. E. Normand, G. Duxbury and N. Langford, *Optics, Comm.* **197**, 115-120 (2001).
10. E. L. Normand, M. T. McCulloch, G. Duxbury and N. Langford, *Optics Letters* **28**, 16-18 (2003)
11. Graham R. Fleming, "chemical Applications of Ultrafast Spectroscopy",Oxford (1986)
12. Ron Bracewell, "The Fourier Transform and Its Applications", McGraw-Hill (1965)
13. J.B McManus, P.L. Keblanian and M.S. Zahniser, *Appl.Opt.* **34**, 3336-3348 (1995)

14. I.F. Howieson, "Near Infrared Tunable Diode Laser Absorption Spectrometer for Trace Gas Detection", PhD Thesis, (1997), University of Strathclyde.
15. Kolmar Technologies photovoltaic HgCdTe photodetector, bandwidth >100MHz
16. Femto Messtechnik 1.1 GHz high speed photodetector amplifier
17. W.J. Lafferty, J.P. Sattler, T.L. Worchesky and K.J. Ritter, *J. Mol. Spectrosc.* **87**, 416-428 (1981)
18. W. Lewis-Bevan, A.J. Merer, M.C.L. Gerry, P.B. Davies, A.J. Morton-Jones and P.A. Hamilton. *J.Mol. Spectrosc*, **113**, 458-471 (1985)
19. E.A. Cohen and W. Lewis-Bevan, *J.Mol. Spectrosc*, **148**, 378-384 (1991)
20. I.S. Rothman, C.P. Rinsland, A. Goldman, T.Massie, D.P. Edwards, J-M. Flaud, A. Perrin, C. Camy-Peyret, V. Dana, J-Y Mandin, J. Schroeder, A. McCann, R.R. Gamache, R.B. Wattson, K. Yoshino, K.V. Chance, K.W. Jucks, L.R. Brown, V. Nemtchinov, and P. Varanas, *JQSRT* **60**, 655-710 (1998).
21. A.G. Maki and J.S. Wells, Wavenumber Calibration Tables from Heterodyne Frequency Measurements (version 1.3) [Online]  
Available:<http://physics.nist.gov/wavenum> [2003,February4]. Originally published as NIST Special Publication 821. National Institute of Standards and Technology, Gaithersburg, MD (1987).

Table 1

Wavenumbers and intensities of absorption lines of nitrous oxide, water and carbon dioxide used for comparison of relative sensitivities of detection in the 8 and 10  $\mu\text{m}$  regions

Molecule	Reference	Transition	Wavenumber/ $\text{cm}^{-1}$	Intensity/( $\text{cm}^{-1}$ molecule $^{-1}$ )
$\text{N}_2\text{O}$	21	$10^0-00^0$ P(32)	1256.3714	6.15E-20
$\text{CO}_2$	20	$10^0-00^0$ R(32)	973.2885	2.29E-23
$\text{H}_2\text{O}$	20	$13_{6,8}-12_{1,11}$	973.4827	3.40E-24

## Figure Captions

### Figure 1

(a) A high resolution absorption spectrum of 1,1 difluoroethylene,  $\text{CF}_2\text{CH}_2$ , recorded, using the QCL as source, with 20 scans of the Bruker Fourier transform IFS 120HR spectrometer at the NERC MSF. The resolution of the spectrometer is  $0.0015\text{ cm}^{-1}$ . The absorption cell had a path length of 26 cm and the gas pressure was 0.9 Torr. The length of the electrical drive pulse applied to the QCL was 200 ns, the pulse repetition frequency, 20 kHz, and the drive current 4.8A. The substrate temperature was  $-1.5\text{ }^\circ\text{C}$ . (i), (ii) and (iii) are three easily identifiable groups of lines.

(b) The upper trace is the absorption spectrum of 1,1 difluoroethylene,  $\text{CF}_2\text{CH}_2$ , recorded using the spectrometer shown in Figure 2. The 36 traversals through the astigmatic Herriott cell gave a path length of 18 m through gas at a pressure of 0.1 Torr. The lower trace is a recording of the etalon fringe pattern of a solid Ge etalon, of nominal fringe spacing  $0.05\text{ cm}^{-1}$ , calibrated fringe spacing  $0.0483\text{ cm}^{-1}$ . The length of the electrical drive pulse applied to the QCL was, 200 ns, the pulse repetition frequency, 5 kHz, and the drive current 4.8A. The temperature of the substrate on which the QCL was mounted was  $-1.52\text{ }^\circ\text{C}$ . The spectrum was recorded using an average of 4096 scans.

## Figure 2

A schematic diagram of the apparatus, the multipass cell used is an astigmatic Herriot cell.

## Figure 3

A trace showing the time dependent amplitude of the emitted pulses of a quantum-cascade laser. (a) The optical path length was 18 m. The drive current was 4.4 A, the pulse length 250 ns, the pulse repetition frequency 500 Hz, and the substrate temperature  $-1.52\text{ }^{\circ}\text{C}$ . (b) The optical path length was 101 m, the drive current was 5 A, the pulse length 300 ns, the pulse repetition frequency 500 Hz, and the substrate temperature  $9.18\text{ }^{\circ}\text{C}$ . In (a) part of the electrical interference associated with the pulse generator may be seen at the start and end of the optical pulse, whereas in (b) the extra time delay between electrical drive pulse and the signal detection minimises the effects of electrical interference both at current switch on and at switch off.

## Figure 4

A comparison of the absorption spectra of the two near oblate top molecules 1,1, difluoroethylene and carbonyl fluoride to show the ease of pattern recognition within a 200 ns time window. Both spectra were recorded using recorded using an average of 4096 scans, an 18 m path length, a 4.2 A drive current and a substrate temperature of

-1.52 °C. (a) 0.051 Torr 1,1, difluoroethylene, (b) 0.055 Torr carbonyl fluoride. The transmission spectra have been off-set for clarity. The wavenumber calibration has been made using the Germanium etalon with fringe spacing 0.0483 cm<sup>-1</sup>, and reference lines of 1,1, difluoroethylene taken from the high resolution Fourier transform spectrum shown in Figure 1(a).

Figure 5: A comparison of the absorption spectra of 1,1, difluoroethylene recorded using two different drive currents. Both spectra were recorded using an average of 4096 scans and an 18 m path length, a substrate temperature of -1.52 °C, and a gas pressure of approximately 0.1 Torr. (a) drive current 4.8 A, average down-chirp -260 MHz/ns, (b) drive current 4.2 A, average down-chirp -214 MHz/ns. The effects of the decreased down-chirp at lower drive voltage may be seen in the increased separation of groups (i) to (iii) at lower voltage, and the greatly improved resolution of groups (ii) and (iii). The transmission spectra have been off set vertically for clarity.

Figure 6: A comparison of a portion the high resolution Fourier transform absorption spectrum of 1,1, difluoroethylene, (recorded using a globar source, with transmission spectra recorded at the end (b) and at the beginning (c) of the laser emission produced of a long 300 ns current pulse. A path length of 101 m, pressure of 0.01 Torr, a drive current of 5 A, and a repetition rate, 500 Hz, were the same for both 6(b) and 6 (c). The shift in

the start wavenumber was produced by temperature tuning, 6(b) used a substrate temperature of -5.52 C shifting the origin to higher wavenumber, and 6(c) a substrate temperature of 9.18 C inducing a shift to lower wavenumber. In (6b), where the average down-chirp is -239.1 MHz/ns, two of the lines in the central cluster with a resolution of  $0.01 \text{ cm}^{-1}$  are just resolved, whereas in 6(c), where the average down-chirp is -285.6 MHz/ns the overall resolution is much poorer, and the resolution of the central structure is lost.

Figure 7: A portion of the atmosphere in the laboratory recorded at reduced pressure using a path length of 101 m. The laser drive current was 5 A, the pulse length 232 ns, the repetition rate 5 kHz, and the substrate temperature  $-1.52 \text{ }^{\circ}\text{C}$ . An average of 64 thousand scans was used. (a) cell pressure 50.5 Torr, (b) pressure 104.5 Torr, (c) carbon dioxide contained in human breath which was added to the sample, the pressure was then reduced to 103.2 Torr. The very weak water line has almost the same percentage absorption in traces (b) and (c). However, it is evident that a large increase in the percentage of absorption due to carbon dioxide has occurred in trace (c) in comparison to trace (b).

Figures (one per page)

Figure 1a

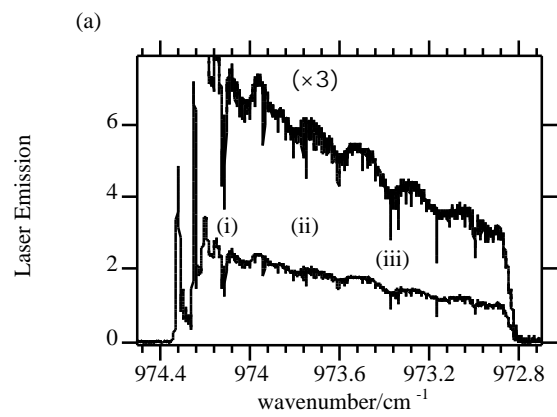


Figure 1 b

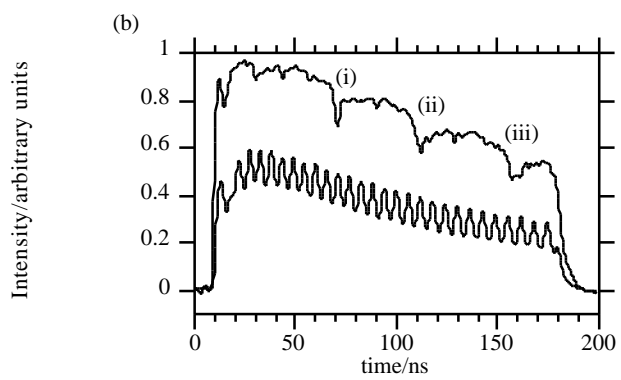


Figure 2

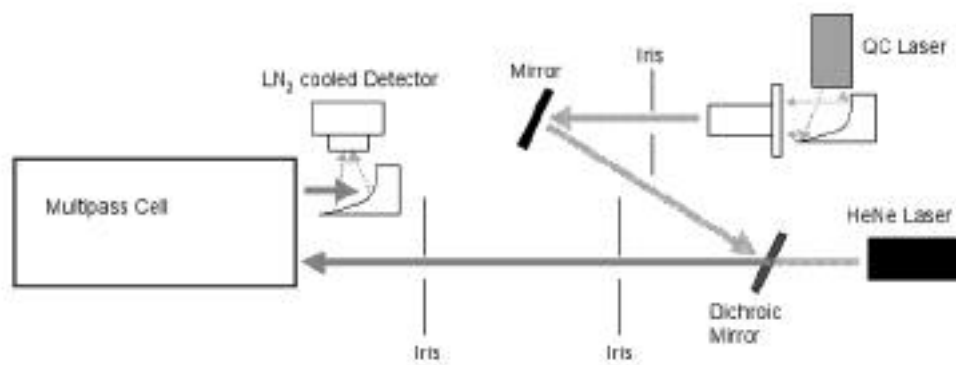


Figure 3a

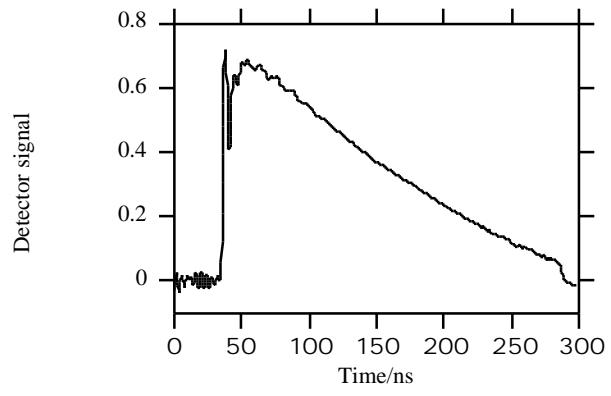


Figure 3b

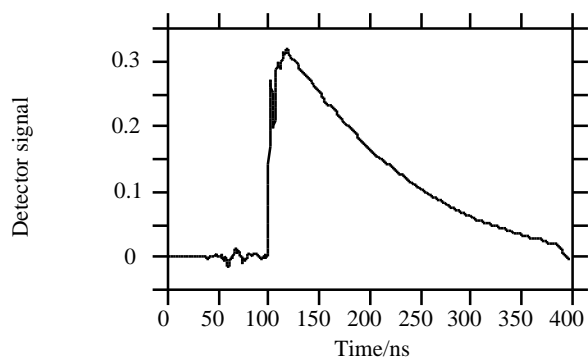


Figure 4

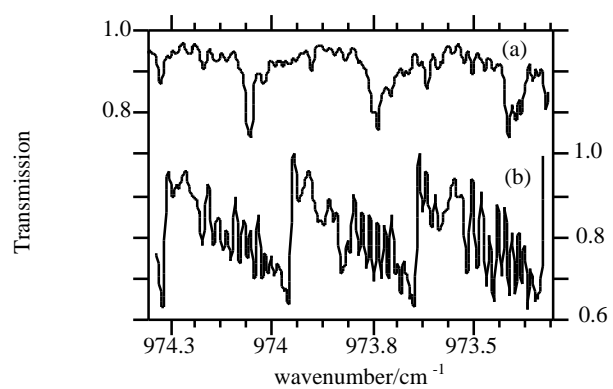


Figure 5

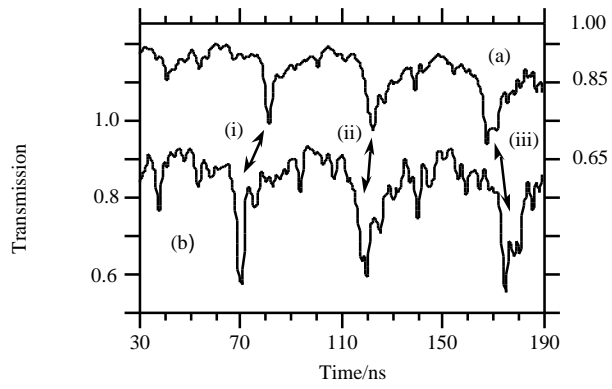


Figure 6a

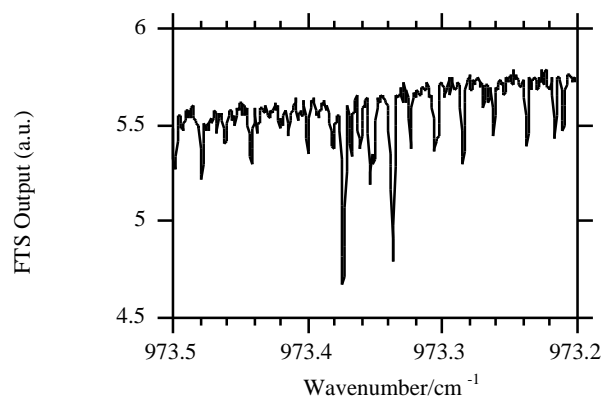


Figure 6b

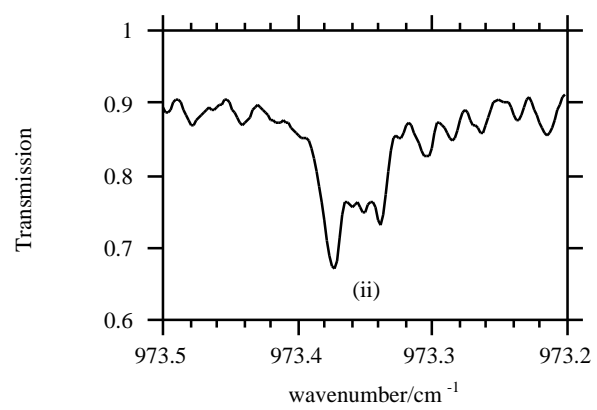


Figure 6c

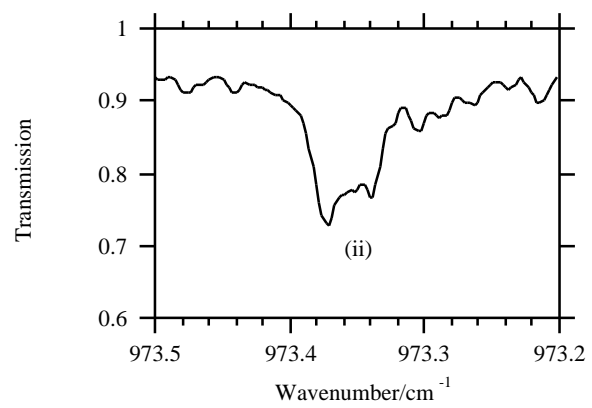


Figure 7

